Aspects of High Scale Leptogenesis with Low Energy CP Violation

S. T. Petcov

SISSA/INFN, Trieste, Italy, and
Kavli IPMU, University of Tokyo, Japan

International Workshop on
High Scale Baryogenesis (on-line workshop)
Kavli IPMU, Tokyo, Japan
January 11, 2022

The origin of the matter-antimatter (or baryon) asymmetry of the Universe is still a fundamental and unresolved problem in Particle Physics and Cosmology, i.e., in Astroparticle Physics. Its solution requires physics beyond that predicted by the Standard Model.

Leptogenesis offers a particularly appealing solution as it relates the generation and smallness of neutrino masses to the generation of the baryon asymmetry of the Universe (BAU).

In its simple realisation a lepton charge CP violating asymmetry is generated in the Early Universe in the CP and lepton charge non-conserving decays of the heavy Majorana neutrinos $N_{1,2,3}$ of the (type I) seesaw mechanism of neutrino mass generation. This asymmetry is converted into a BAU by (B+L) violating but (B-L) conserving sphaleron processes which exist in the SM and are effective at $T \sim (132 - 10^{12})$ GeV. The generation of BAU takes place approximately at $T \sim M_1$, assuming $M_1 < M_2 < M_3$, M_i being the mass of N_i.

In

K. Moffat, S. Pascoli, S.T.P., H. Schulz, J. Turner, arXiv:1804.05066 (Phys. Rev. D98 (2018) 015036),

K. Moffat, S. Pascoli, S.T.P., J. Turner, arXiv:1809.08251 (JHEP 03 (2019) 034),

I. Brivio, K. Moffat, S. Pascoli, S.T.P., arXiv:1905.12642 (JHEP 10 (2019) 059),

A. Granelli, K. Moffat, S.T.P., arXiv:2107.02079 (JHEP 11(2021) 149),

we have addressed the following questions:

A. How low can be the scale of non-resonant leptogenesis (LG) in the general case (i.e., in the absence of further specific (symmetry) conditions or constraints on the spectrum of masses of $N_{1,2,3}$)?

B. How low/high can be the scale of non-resonant leptogenesis (LG) in the general case (no specific additional conditions on $M_{1,2,3}$) when the requisite CP violation in LG is provided exclusively by the CP violating Dirac or Majorana phases in the PMNS neutrino mixing matrix?

C. Is leptogenesis compatible with the Neutrino Option in general and in the case of low-energy leptonic CP violation?

D. How the transitions between the different LG flavour regimes occur when the requisite CPV is due exclusively to the leptonic Dirac or Majorana CPV phases?

Neutrino Masses, Mixing, Seesaw Mechanism

Reference Model: 3 light ν mixing

$$\nu_{l\mathsf{L}} = \sum_{j=1}^{3} U_{lj}\,\nu_{j\mathsf{L}} (+ \sum_{k=1}^{3} V_{lk}\,N_{k\mathsf{L}})\,, \quad l = e, \mu, \tau.$$

The PMNS matrix U (practically) - 3×3 unitary ($|V_{lk}| <<< 1$).

ν_j, $m_j \neq 0$: (Dirac or) Majorana particles.

(N_k - heavy Majorana neutrinos, $M_k \gtrsim 10^6$ GeV.)

Data: 3 νs are light: $\nu_{1,2,3}$, $m_{1,2,3} \lesssim 0.5$ eV.

3-ν mixing: 3-flavour neutrino oscillations possible.

ν_μ, E; at distance L: $P(\nu_\mu \to \nu_{\tau(e)}) \neq 0$, $P(\nu_\mu \to \nu_\mu) < 1$

$P(\nu_l \to \nu_{l'}) = P(\nu_l \to \nu_{l'}; E, L; U; m^2_2 - m^2_1, m^2_3 - m^2_1)$

PMNS Matrix: Standard Parametrization

$$U = V\,P\,, \qquad P = \begin{pmatrix} 1 & 0 & 0 \\ 0 & e^{i\frac{\alpha_{21}}{2}} & 0 \\ 0 & 0 & e^{i\frac{\alpha_{31}}{2}} \end{pmatrix}\,,$$

$$V = \begin{pmatrix} c_{12}c_{13} & s_{12}c_{13} & s_{13}e^{-i\delta} \\ -s_{12}c_{23} - c_{12}s_{23}s_{13}e^{i\delta} & c_{12}c_{23} - s_{12}s_{23}s_{13}e^{i\delta} & s_{23}c_{13} \\ s_{12}s_{23} - c_{12}c_{23}s_{13}e^{i\delta} & -c_{12}s_{23} - s_{12}c_{23}s_{13}e^{i\delta} & c_{23}c_{13} \end{pmatrix}$$

- $s_{ij} \equiv \sin\theta_{ij}$, $c_{ij} \equiv \cos\theta_{ij}$, $\theta_{ij} = [0, \frac{\pi}{2}]$,
- δ - Dirac CPV phase, $\delta = [0, 2\pi]$; CP inv.: $\delta = 0, \pi, 2\pi$;
- α_{21}, α_{31} - Majorana CPV phases; CP inv.: $\alpha_{21(31)} = k(k')\pi$, $k(k') = 0, 1, 2...$

  S.M. Bilenky et al., 1980
- $\Delta m^2_{\odot} \equiv \Delta m^2_{21} \cong 7.34 \times 10^{-5}$ eV$^2 > 0$, $\sin^2\theta_{12} \cong 0.305$, $\cos 2\theta_{12} \gtrsim 0.306$ (3σ),
- $|\Delta m^2_{31(32)}| \cong 2.448\ (2.502) \times 10^{-3}$ eV^2, $\sin^2\theta_{23} \cong 0.545\ (0.551)$, NO (IO) ,
- θ_{13} - the CHOOZ angle: $\sin^2\theta_{13} = 0.0222\ (0.0223)$

  F. Capozzi et al. (Bari Group), arXiv:2003.08511.

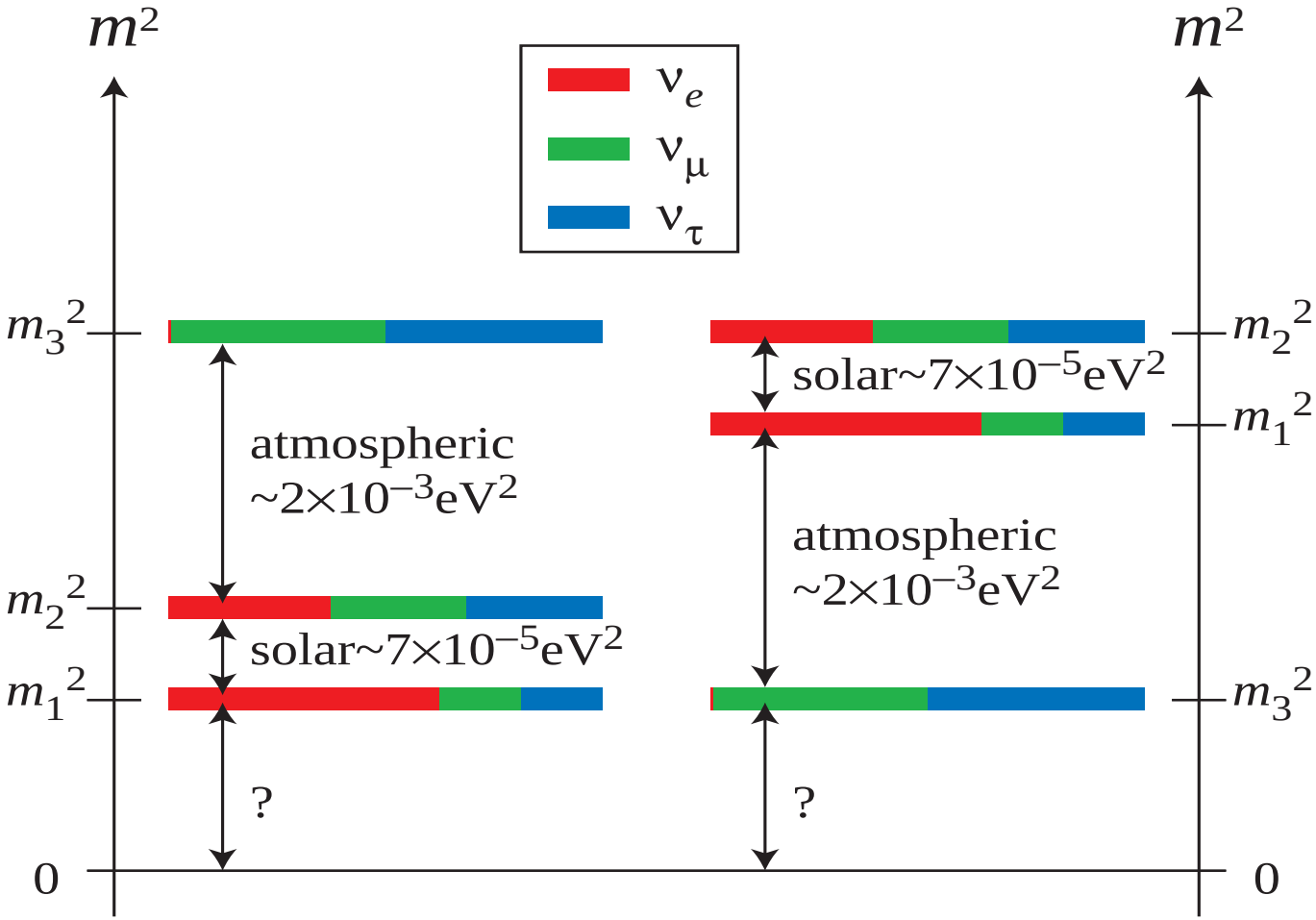

NO: $\Delta m^2_{31(32)} > 0$, $m_1 < m_2 < m_3$;
IO: $\Delta m^2_{31(32)} < 0$, $m_3 < m_1 < m_2$.

- Dirac phase δ: $\nu_l \leftrightarrow \nu_{l'}$, $\bar{\nu}_l \leftrightarrow \bar{\nu}_{l'}$, $l \neq l'$; $A_{\rm CP}^{(l,l')} \propto J_{\rm CP} \propto \sin\theta_{13}\sin\delta$:

P.I. Krastev, S.T.P., 1988

$$J_{CP} = \text{Im}\left\{U_{e1}\, U_{\mu 2}\, U_{e2}^{*}\, U_{\mu 1}^{*}\right\} = \frac{1}{8}\sin 2\theta_{12}\sin 2\theta_{23}\sin 2\theta_{13}\cos\theta_{13}\sin\delta$$

Current data: $|J_{CP}| \lesssim 0.035$ (can be relatively large!); b.f.v. with $\delta = 3\pi/2$: $J_{CP} \cong -0.035$.

- Majorana phases α_{21}, α_{31}:
  - $\nu_l \leftrightarrow \nu_{l'}$, $\bar{\nu}_l \leftrightarrow \bar{\nu}_{l'}$ not sensitive;

S.M. Bilenky et al., 1980;
P. Langacker et al., 1987

  - $|<m>|$ in $(\beta\beta)_{0\nu}$–decay depends on α_{21}, α_{31};
  - $\Gamma(\mu \to e + \gamma)$ etc. in SUSY theories depend on $\alpha_{21,31}$;
  - BAU, leptogenesis scenario: $\delta, \alpha_{21,31}$!

Global analyses after Nu2020: combine latest T2K and NOνA data.

Results on CPV due to δ and NO vs IO spectrum - inconclusive.

K.J. Kelly, P.A. Machado, S.J. Parke, Y.F. Perez Gonzalez and R. Zukanovich-Funchal,
"Back to (Mass-)Square(d) One: The Neutrino Mass Ordering in Light of Recent Data," arXiv:2007.08526 [hep-ph].

I. Esteban, M.C. Gonzalez-Garcia, M. Maltoni, T. Schwetz and A. Zhou, "The fate of hints: updated global analysis of three-flavor neutrino oscillations," arXiv:2007.14792 [hep-ph].

Result on CPV, b.f.v.: $\delta = 197°$, NO; $\delta = 282°$, IO.

At 3σ: δ is found to lie in $[120°, 369°]$ ($[193°, 352°]$), NO (IO).

IO: CPV due to δ at 3σ.

IO disfavored at 1.6σ with respect to NO (2.7σ including SuperK ν_{atm} data).

Ordering	θ_{12} ($^\circ$)	θ_{13} ($^\circ$)	θ_{23} ($^\circ$)	δ ($^\circ$)	$\Delta m^2_\odot$ (10^{-5} eV^2)	$\Delta m^2_{\rm atm}$ (10^{-3} eV^2)
NO	$33.44^{+0.77}_{-0.74}$	$8.57^{+0.12}_{-0.12}$	$49.2^{+0.9}_{-1.2}$	197^{+27}_{-24}	$7.42^{+0.21}_{-0.20}$	$2.517^{+0.026}_{-0.028}$
IO	$33.45^{+0.78}_{-0.75}$	$8.60^{+0.12}_{-0.12}$	$49.3^{+0.9}_{-1.1}$	282^{+26}_{-30}	$7.42^{+0.21}_{-0.20}$	$-2.498^{+0.028}_{-0.028}$

Best-fit values and 1σ allowed ranges of the neutrino mixing angles θ_{12}, θ_{13}, θ_{23}, and of the $\Delta m^2_\odot \equiv \Delta m^2_{21}$ and $\Delta m^2_{\rm atm} \equiv \Delta m^2_{31}$ ($\Delta m^2_{\rm atm} \equiv \Delta m^2_{32}$) in the case of NO (IO) light neutrino mass spectrum, obtained in I. Esteban et al., arXiv:2007.14792. We quote also the best-fit value and 1σ allowed ranges of the Dirac CPV phase δ from I. Esteban et al., arXiv:2007.14792 However, these data on δ are not used in our analyses.

$$\mathcal{L}_{\mathrm{Y,M}}(\mathbf{x}) = -\left(\mathbf{Y}_{\alpha \mathrm{i}}\overline{\psi_{\alpha \mathbf{L}}}(\mathbf{x})\,\mathbf{i}\tau_2\,\mathbf{\Phi}^*(\mathbf{x})\,\mathbf{N}_{\mathbf{iR}}(\mathbf{x}) + \mathrm{h.c.}\right) - \frac{\mathbf{1}}{\mathbf{2}}\mathbf{M}_{\mathbf{i}}\,\overline{\mathbf{N}_{\mathbf{i}}}(\mathbf{x})\,\mathbf{N}_{\mathbf{i}}(\mathbf{x})\,,$$

$Y_{\alpha i}$ **– the matrix of the neutrino Yukawa coupling,**
$N_i(x) = N_{iR}(x) + N^c_{iL}(x) = C(\overline{N_i}(x))^T$**,** $N^c_{iL}(x) \equiv C(\overline{N_{iR}}(x))^T$**,** $C^{-1}\gamma_\mu C = -\gamma^T_\mu$**.**
$N_{1,2,3}(x)$ **– heavy Majorana neutrinos** $N_{1,2,3}$**,** $M_{1,2,3} > 0$**. In high scale leptogenesis** $M_{1,2,3} \sim (10^6 - 10^{14})$ **GeV.**

After the SBEWS,

$$\mathcal{L}^m_\nu = -\frac{1}{2}\left(\overline{\nu_{\alpha L}} \quad \overline{N^c_{iL}}\right)\begin{pmatrix} O_{\alpha\beta} & \frac{v}{\sqrt{2}}Y_{\alpha j} \\ \frac{v}{\sqrt{2}}(Y^T)_{i\beta} & M_i\delta_{ij}\end{pmatrix}\begin{pmatrix}\nu^c_{\beta R} \\ N_{jR}\end{pmatrix} + h.c.\,, \qquad v = 246 \text{ GeV}\,,$$

$\alpha,\,\beta = e,\,\mu,\,\tau$ **(**$i,\,j = 1,\,2,\,3$**),** $\nu^c_{\beta R}(x) \equiv C(\overline{\nu_{\beta L}}(x))^T$**.**

Can be diagonalised by means of the Takagi transformation; at leading order in $|vY_{\alpha i}|/M_i \ll 1$**, leads to the well known seesaw expression for the tree-level light neutrino mass matrix** $m_\nu^{\mathbf{tree}}$**:**

$$\left(m_\nu^{\mathbf{tree}}\right)_{\alpha\beta} \cong -\frac{v^2}{2}Y_{\alpha i}\;M_i^{-1}\left(Y^T\right)_{i\beta}.$$

Casas-Ibarra Parametrisation

One-loop contribution to m_ν:

$$(m_\nu^{\textbf{1-loop}})_{\alpha\beta} = Y_{\alpha i}\ \frac{M_i}{32\pi^2}\left(\frac{\log\left(M_i^2/m_H^2\right)}{M_i^2/m_H^2-1}+3\frac{\log\left(M_i^2/m_Z^2\right)}{M_i^2/m_Z^2-1}\right)\left(Y^T\right)_{i\beta}\,,$$

$m_H = 125$ **GeV,** $m_Z = 91.2$ **GeV.**

A. Pilaftsis, hep-ph/9901206; D. Aristizabal Sierra, C. Yaguna, arXiv:1106.3587; J. Lopez-Pavon, S. Pascoli, C.-F. Wong, arXiv:1209.5342

The light neutrino mass matrix including the one-loop correction reads:

$$(m_\nu)_{\alpha\beta} \equiv \left(m_\nu^{\textbf{tree}} + m_\nu^{\textbf{1-loop}}\right)_{\alpha\beta} = -\frac{v^2}{2}\,Y_{\alpha i}\ f(M_i)\left(Y^T\right)_{i\beta}\,,$$

$$f(M_i) \equiv M_i^{-1} - \frac{M_i}{16\pi^2 v^2}\left(\frac{\log\left(M_i^2/m_H^2\right)}{M_i^2/m_H^2-1}+3\frac{\log\left(M_i^2/m_Z^2\right)}{M_i^2/m_Z^2-1}\right)\,.$$

$$\widehat{m}_\nu = U^\dagger m_\nu U^*\,,\quad \widehat{m}_\nu \equiv \textbf{diag}(m_1,\,m_2,\,m_3)\,.$$

The Casas-Ibarra parametrisation of $Y_{\alpha j}$ has the form:

$$Y_{\alpha j} = \pm i\frac{\sqrt{2}}{v}U_{\alpha a}\sqrt{m_a}R_{ja}\sqrt{f^{-1}(M_j)}\,,\quad R^T = R\,,\ \text{complex}\quad (f^{-1}(M_j)\to M_j)\,.$$

J. Lopez-Pavon, E. Molinaro, STP, arXiv:1506.05296

We use the following parametrisation of the R-matrix:

$$R = \begin{pmatrix} 1 & 0 & 0 \\ 0 & c_1 & s_1 \\ 0 & -s_1 & c_1 \end{pmatrix} \begin{pmatrix} c_2 & 0 & s_2 \\ 0 & 1 & 0 \\ -s_2 & 0 & c_2 \end{pmatrix} \begin{pmatrix} c_3 & s_3 & 0 \\ -s_3 & c_3 & 0 \\ 0 & 0 & 1 \end{pmatrix},$$

$c_j \equiv \cos(x_j + iy_j)$ **and** $s_j \equiv \sin(x_j + iy_j)$**,** x_j **and** y_j **being free real parameters** ($j = 1, 2, 3$)**.**

High Scale Leptogenesis

Boltzmann Equations vs. Density Matrix Formalism

In high scale LG, based on type I seesaw, the out-of-equilibrium decays $N_j \to l^+ + \Phi^{(-)}$ and $N_j \to l^- + \Phi^{(+)}$ of N_j, caused by the CPV $Y_{\alpha i}$ proceed with different rates, producing CPV asymmetries $\Delta L_l \neq 0$ and $\Delta L \neq 0$ in L_l, $l = e, \mu, \tau$ and $L = L_e + L_\mu + L_\tau$ of the Universe.
$\Delta L_l \neq 0$ and $\Delta L \neq 0$ are converted into a baryon asymmetry by $(B - L)$-conserving, but $(B + L)$-violating, sphaleron processes which exist in the SM and are effective at temperatures $T \sim (132 - 10^{12})$ GeV.
The values of the masses M_i of N_i set the scale of LG.

The charged lepton final states in the decays of the heavy neutrino N_i, $N_i \to \Phi^+ \psi_i$ and $N_i \to \Phi^- \overline{\psi_i}$, are a superposition of the charged lepton flavour states, namely,

$$|\psi_i\rangle = \sum_{\alpha=e,\,\mu,\,\tau} C_{i\alpha} |\psi_\alpha\rangle \,, \quad |\overline{\psi_i}\rangle = \sum_{\alpha=e,\,\mu,\,\tau} \overline{C}^*_{i\alpha} |\overline{\psi_\alpha}\rangle \,,$$

$$C_{i\alpha} = \overline{C}_{i\alpha} = \frac{Y_{\alpha i}}{\sqrt{(Y^\dagger Y)_{ii}}} \,.$$

We consider for simplicity the decays of N_1, $N_1 \to \Phi^+ \psi_1$ and $N_1 \to \Phi^- \overline{\psi_1}$.

Without the SM charged lepton Yukawa interactions, $\mathcal{L}^l_Y$, $|\psi_1\rangle$, $|\overline{\psi_1}\rangle$ – coherent superpositions of $|\psi_\alpha\rangle$, $|\overline{\psi_\alpha}\rangle$, $\alpha = e, \mu, \tau$, the flavour states are not distinguishable.

When $\mathcal{L}^l_Y$ – in thermal equilibrium, $|\psi_e\rangle$, $|\psi_\mu\rangle$, $|\psi_\tau\rangle$ ($|\overline{\psi_e}\rangle$, $|\overline{\psi_\mu}\rangle$, $|\overline{\psi_\tau}\rangle$) – distinguishable since charged lepton Yukawa couplings $h_e << h_\mu << h_\tau$.

If $\mathcal{L}^l_Y$ are faster than $N_1 \to \Phi^+ \psi_1$, $N_1 \to \Phi^- \overline{\psi_1}$, the coherence in $|\psi_1\rangle$ ($|\overline{\psi_1}\rangle$) – destroyed. $\mathcal{L}^l_Y$ – source of decoherence effects.

$\Gamma_{\tau,\,\mu,e} \cong 8 \times 10^{-3} h^2_{\tau,\,\mu,\,e}\; T$,

$h_\tau = \frac{\sqrt{2}}{v} m_\tau \cong 1.02 \times 10^{-2}$, $h_\mu = \frac{\sqrt{2}}{v} m_\mu \cong 6.08 \times 10^{-4}$,
$h_e = \frac{\sqrt{2}}{v} m_e \cong 2.94 \times 10^{-6}$.

The comparison of $\Gamma_{\tau,\mu,e}$ with the Hubble expansion rate H gives:

$$\frac{\Gamma_\tau}{H} \cong \frac{M_P}{T}\; 4.85 \times 10^{-8} \cong \left(\frac{1\ \text{GeV}}{T}\right)\; 5.92 \times 10^{11}\,,$$
$$\frac{\Gamma_\mu}{H} \cong \frac{M_P}{T}\; 1.72 \times 10^{-10} \cong \left(\frac{1\ \text{GeV}}{T}\right)\; 2.10 \times 10^{9}\,,$$
$$\frac{\Gamma_e}{H} \cong \frac{M_P}{T}\; 0.43 \times 10^{-14} \cong \left(\frac{1\ \text{GeV}}{T}\right)\; 0.52 \times 10^{5}\,,$$

$M_P \cong 1.22 \times 10^{19}$ **GeV is the Planck mass,**
$H(T) = (2\pi T^2/(3M_P))\sqrt{g_*\pi/5}$, $g_* \cong 106.75$.

Thus, Γ_τ, Γ_μ, Γ_e - relevant at $T \lesssim 10^{12}$, 10^9, 10^5 GeV.

Boltzmann equations: semi-classical, time-evolution of the number densities of N_1 and $B-L$ charge of the Universe.

Valid

i) at $T \sim M_1 \gg 10^{12}$ GeV where $\Gamma_l(M_1)/H(M_1) \ll 1$,
provied the decoherence effects due to $\Gamma_{\tau,\mu,e}$ are neglected:
unflavoured or single-flavour regime, leptogenesis (N_1: 1BE1F);

ii) at $10^9 < T \sim M_1 \lesssim 10^{12}$ GeV, $\Gamma_\tau/H(M_1) \gtrsim 1$ ($\Gamma_{\mu,e}/H(M_1) \ll 1$, set to 0),
provided $\mathcal{L}^\tau_Y$-mediated interactions are infinitely ($\equiv$ "sufficiently") fast during the whole period of LG:
two-flavoured regime, leptogenesis (N_1: 1BE2F);

iii) at $T \sim M_1 < 10^9$ GeV, where $\Gamma_\tau/H(M_1) \gg 1$, $\Gamma_\mu/H(M_1) \gtrsim 1$,
provided $\mathcal{L}^\tau_Y$- and $\mathcal{L}^\mu_Y$ mediated interactions are infinitely ($\equiv$ "sufficiently") fast during the whole period of LG: three-flavoured regime,leptogenesis (N_1: 1BE3F).

At $T \gg 10^{12}$ GeV, $\Gamma_l/H(T) \ll 1$, charged lepton flavour states are indistinguishable, $|\psi_1\rangle$ ($|\overline{\psi_1}\rangle$) from N_1 decay – coherent superpositions of $|\psi_\alpha\rangle$ ($|\overline{\psi_\alpha}\rangle$), $\alpha = e, \mu, \tau$,

$\Gamma_{\tau,\mu}$ decoherence effects - neglected: unflavoured or single-flavour regime, unflavoured or single-flavoured leptogenesis.
The time-evolution of the number densities of N_1 and $B-L$ charge can be described by the set of semi-classical single-flavoured Boltzmann equations (1BE1F):

$$\begin{aligned} \frac{dN_{N_1}}{dz} &= -D_1 \left(N_{N_1} - N^{eq}_{N_1}\right) , \\ \frac{dN_{B-L}}{dz} &= \epsilon^{(1)} D_1 \left(N_{N_1} - N^{eq}_{N_1}\right) - W_1 N_{B-L} , \end{aligned}$$

$z \equiv M_1/T$, the decay parameter $D_1(z) = \kappa_1 z \frac{K_1(z)}{K_2(z)}$, $\kappa_1 = \Gamma^{(0)}_{N_1}/H(T = M_1)$, $\Gamma^{(0)}_{N_1} = (Y^\dagger Y)_{11} M_1/8\pi$ – N_1 total decay rate at $T = 0$, $N^{eq}_{N_1}(z) = \frac{3}{8} z^2 K_2(z)$, $K_n(z)$, $n = 1, 2, ...$, is the modified n^{th} Bessel function of the 2nd kind; the wash-out parameter $W_1 = D_1(z)\, N^{eq}_{N_1}(z)/(2N^{eq}_\ell(z = 0))$, ($N^{eq}_\ell(z = 0) = 3/4$).

The CPV-asymmetry parameter $\epsilon^{(1)}$:

$$\epsilon^{(1)} = \frac{3}{16\pi (Y^\dagger Y)_{11}} \sum_{j\neq 1} \Im\left[(Y^\dagger Y)^2_{1j}\right] \frac{\xi(x_j)}{\sqrt{x_j}}\,, \quad x_j \equiv M_j^2/M_1^2\,,$$

$$\xi(x) \equiv \frac{2}{3} x \left[(1+x)\log\left(1+\frac{1}{x}\right) - \frac{2-x}{1-x}\right]\,.$$

Since the Yukawas enter in $\epsilon^{(1)}$ only through the product $Y^\dagger Y$, there is no dependence on the PMNS matrix. There is therefore no contribution to $\epsilon^{(1)}$ from the CPV Dirac and Majorana phases in the PMNS matrix.

Boltzmann equations cannot describe the transitions between the different flavour regimes in leptogenesis: decoherence effects neither infinetely fast nor negligible; may not describe correctly the generation of BAU in a given flavour regime.

The density matrix equations (DMEs) – accurate tool to study thermal LG accounting for quantum decoherence processes as their effects change continuously in time (at T decreases).

The DMEs describe the time-evolution of the entries of the density matrix :

$$N = \sum_{\alpha,\beta} N_{\alpha\beta} |\psi_\alpha\rangle\langle\psi_\beta| \,, \quad \alpha,\, \beta = e,\, \mu,\, \tau \,.$$

$N_{\alpha\alpha}$ **– the number density of** $\frac{1}{3}B - L_\alpha$ **asymmetry,** $N_{B-L} = \mathbf{Tr}(N) = \sum_\alpha N_{\alpha\alpha}$**.**

$N_{\alpha\beta}$**,** $\alpha \neq \beta$**, describe the degree of coherence between the flavour states.**

The DMEs in the three-flavour basis explicitly read:

$$\begin{aligned}
\frac{dN_{N_1}}{dz} &= -D_1(N_{N_1} - N_{N_1}^{\mathbf{eq}}) \\
\frac{dN_{\alpha\beta}}{dz} &= \epsilon^{(1)}_{\alpha\beta} D_1(N_{N_1} - N_{N_1}^{\mathbf{eq}}) - \frac{1}{2} W_1 \left\{P^{0(1)}, N\right\}_{\alpha\beta} \\
&\quad -\frac{\Gamma_\tau}{Hz}\left[I_\tau, [I_\tau, N]\right]_{\alpha\beta} - \frac{\Gamma_\mu}{Hz}\left[I_\mu, [I_\mu, N]\right]_{\alpha\beta} \,,
\end{aligned}$$

A. De Simone, A. Riotto, hep-ph/0611357; S. Blanchet, P.D. Bari and G.G. Raffelt, hep-ph/0611337; S. Blanchet et al., arXiv:1112.4528

I_τ **and** I_μ **are** 3×3 **matrices,**$(I_\tau)_{\alpha\beta} = \delta_{\alpha\tau}\delta_{\beta\tau}$**,**$(I_\mu)_{\alpha\beta} = \delta_{\alpha\mu}\delta_{\beta\mu}$**,**

$$P^{0(1)}_{\alpha\beta} \equiv C_{1\alpha} C^*_{1\beta} \,, \quad \text{(projection matrices)} \,.$$

The anti-commutator structure

$$\left\{P^{0(1)}, N\right\}_{\alpha\beta} = \sum_{\gamma=e,\,\mu,\,\tau} \left(C_{1\alpha} C^*_{1\gamma} N_{\gamma\beta} + C_{1\gamma} C^*_{1\beta} N_{\alpha\gamma}\right) \,.$$

The double-commutator structures in the equation for $dN_{N_{\alpha\beta}}/dz$ **give rise to an exponentially damping term proportional to** $\Gamma_{\tau,\,\mu}/Hz$ **for the equations describing the density matrix off-diagonal elements** $N_{\alpha\beta}$**. If these terms are infinitely large, i.e.,** $\Gamma_{\tau,\,\mu} \to +\infty$**, the density matrix is driven towards a diagonal form and the DMEs reduce to the three-flavoured set of Boltzmann equations 1BE3F.**

The CPV-asymmetry:

$$\epsilon^{(1)}_{\alpha\beta} = \frac{3}{32\pi \left(Y^\dagger Y\right)_{11}} \sum_{j\neq 1} \Big\{ i \left[Y_{\alpha 1} Y^*_{\beta j} (Y^\dagger Y)_{j1} - Y^*_{\beta 1} Y_{\alpha j} (Y^\dagger Y)_{1j} \right] f_1\left(x_j\right)$$

$$+ i \left[Y_{\alpha 1} Y^*_{\beta j} (Y^\dagger Y)_{1j} - Y^*_{\beta 1} Y_{\alpha j} (Y^\dagger Y)_{j1} \right] f_2\left(x_j\right) \Big\}, \;\; x_j \equiv M_j^2/M_1^2 \,,$$

$$f_1\left(x\right) \equiv \frac{\xi\left(x\right)}{\sqrt{x}} \,, \qquad f_2\left(x\right) \equiv \frac{2}{3\left(x-1\right)} \,.$$

In the numerical analyses that follow, we will use the ULYSSES Python package (A. Granelli, K. Moffat, Y. Perez-Gonzalez, H. Schulz and J. Turner, arXiv:2007.09150) to solve the DME.
The code computes $N_{B-L} = N_{ee} + N_{\mu\mu} + N_{\tau\tau}$, which is then converted into BAU η_B (expressed in terms of the baryon-to-photon ratio):

$$\eta_B = \frac{28}{79} \frac{1}{27} N_{B-L} \,,$$

$28/79$ is the SM sphaleron conversion coefficient; the $1/27$ factor comes from the dilution of the baryon asymmetry due to the change of the photon density between leptogenesis and recombination.

Baryon Asymmetry

$$Y_B = \frac{n_B - n_{\bar{B}}}{n_\gamma} = (6.10 \pm 0.04) \times 10^{-10}\,, \qquad \textbf{CMB}$$

P.A.R. Ade et al. (Planck Collab.), arXiv:1502.01589

A. The Davidson-Ibarra bound (hep-ph/0202239): successful LG possible for

$T \sim M_1 \gtrsim 10^9$ **GeV**

Assumed $M_1 \ll M_2 \ll M_3$; flavour effects not included.

K. Moffat et al., arXiv:1804.05066

Successful LG possible for

$T \sim M_1 = 10^6$ **GeV,** $M_2 \cong 3M_1$, $M_3 \cong 3M_2$

Three-flavour LG; density matrix fromalism; 11-dim parameter space scanned (θ_{23}, δ, $\alpha_{21,31}$, m_1, 6 Casas-Ibarra matrix parameters)

May require fine tuning; for $M_1 < 10^6$ GeV the fine tuning is "exceedingly" large.

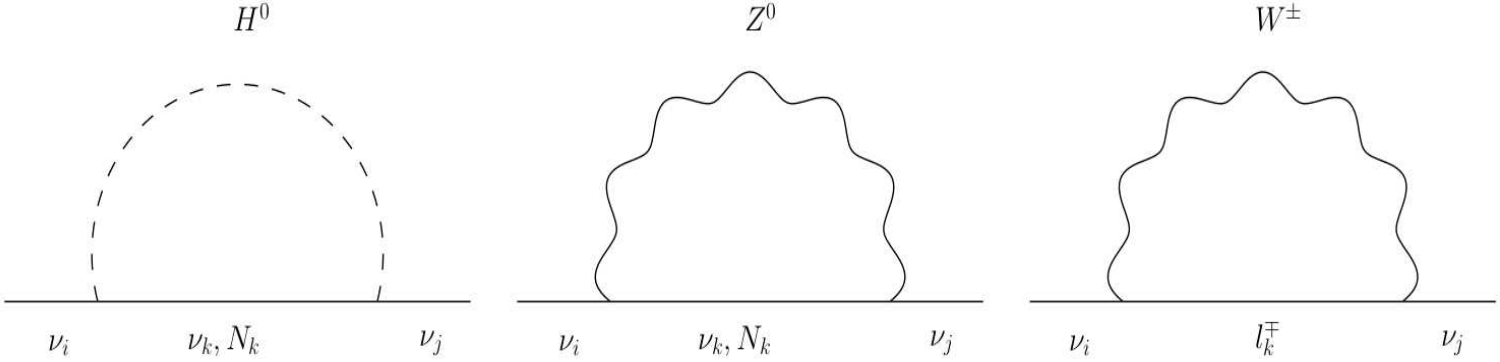

$$m_\nu = m^{\textbf{tree}} + m^{\textbf{1-loop}}.$$

$$m^{\textbf{tree}} \approx m_D M^{-1} m_D^T\,, \quad m_D = vY\,,$$

$$m^{\textbf{1-loop}} = -\frac{1}{32\pi^2 v^2} m_D \textbf{diag}\left(g\left(M_1\right), g\left(M_2\right), g\left(M_3\right)\right) m_D^T,$$

$$g\left(M_i\right) \equiv M_i \left(\frac{\log\left(\frac{M_i^2}{m_H^2}\right)}{\frac{M_i^2}{m_H^2} - 1} + 3 \frac{\log\left(\frac{M_i^2}{m_Z^2}\right)}{\frac{M_i^2}{m_Z^2} - 1} \right)$$

	$\theta_{23}(^\circ)$	$\delta(^\circ)$	$\alpha_{21}(^\circ)$	$\alpha_{31}(^\circ)$	$x_1(^\circ)$	$y_1(^\circ)$	$x_2(^\circ)$	$y_2(^\circ)$	$x_3(^\circ)$	$y_3(^\circ)$	$m_{1(3)}$ (eV)	M_1 (GeV)	M_2 (GeV)	M_3(GeV)
S_1	46.24	281.21	181.90	344.71	132.23	179.88	87.81	2.88	-30.25	177.5	0.120	$10^{6.0}$	$10^{6.5}$	$10^{7.0}$
S_2	46.57	88.26	116.07	420.44	44.36	171.78	86.94	2.96	97.01	174.30	0.079	$10^{6.5}$	10^{7}	$10^{7.5}$
S_3	46.63	31.71	130.95	649.65	-72.33	170.54	86.96	2.22	-1.86	178.31	0.114	$10^{6.5}$	$10^{7.2}$	$10^{7.9}$
$\overline{S_1}$	40.56	158.51	157.48	511.0	-16.23	179.29	90.04	1.29	-107.14	179.22	0.0047	$10^{6.0}$	$10^{6.5}$	$10^{7.0}$
$\overline{S_2}$	43.67	201.02	238.77	658.33	-39.88	178.68	88.12	2.46	53.97	158.01	0.0133	$10^{6.5}$	$10^{7.0}$	$10^{7.5}$
$\overline{S_3}$	43.64	57.28	179.87	292.95	86.58	174.40	91.11	1.61	134.48	173.74	0.012	$10^{6.5}$	$10^{7.2}$	$10^{7.9}$
$F.T^{\text{loop}}$	44.59	140.04	537.15	291.89	164.06	-149.85	178.99	49.15	93.39	-14.50	0.15882	$10^{9.0}$	$10^{9.5}$	10^{10}
$F.T^{\text{tree}}$	43.81	31.59	681.96	276.19	271.56	-125.27	14.95	-11.50	344.87	5.22	0.0041	$10^{9.0}$	$10^{9.5}$	10^{10}

The best-fit points for the leptogenesis scenarios are given and are all consistent with $\eta_B = (6.10 \pm 0.04) \times 10^{-10}$, $\theta_{13} = 8.52^\circ$ and $\theta_{12} = 33.63^\circ$. The upper (lower) three rows are the best-fit points for normal (inverted) ordering. The final two rows are the best fit points for normal ordering in the loop and tree-level dominated scenarios.

$R-$matrix parameters: $R = R_{23}(\omega_1)\, R_{13}(\omega_2)\, R_{12}(\omega_3)$

$\omega_j = x_j + i y_j$, $\omega_1 = \omega_{23}$, $\omega_2 = \omega_{13}$, $\omega_3 = \omega_{12}$.

B. How low/high can be the scale of non-resonant leptogenesis (LG) in the general case (no specific additional conditions on $M_{1,2,3}$) when the requisite CP violation in LG is provided exclusively by the CP violating Dirac (δ) or Majorana ($\alpha_{21,31}$) phases in the PMNS neutrino mixing matrix?

2006: N_1, N_2, $M_1 \ll M_2$, 2-flavour LG, $M_1 \lesssim 5 \times 10^{11}$ GeV, Dirac CPV, CP conserving Casas-Ibarra matrix R,

$$|\sin\theta_{13}\,\sin\delta| \gtrsim 0.09$$

S. Pascoli, STP, A. Riotto hep-ph/0611338

K. Moffat et al., arXiv:1809.08251 (JHEP 03 (2019) 034)

2018: N_1, N_2, N_3, $M_1 < M_2 < M_3$, 3-flavour and 2-flavour regimes investigated, assumed CP conserving R-matrix (= real or purely imaginary elements).

Confirmed the 2006 PPR result.

Thermal LG viable for $10^6 \lesssim T \cong M_1 \lesssim 10^{13}$ GeV.

At $T \cong M_1 \sim 10^6$ GeV, "fine tuning" of the light neutrino masses necessary (as discussed in A.).

Results presented for $M_1 < 10^9$ GeV:
$M_1 = 3.16 \times 10^6,\ 1.29 \times 10^8,\ 7 \times 10^8$ **GeV,**
$M_2 = 3.5 M_1$, $M_3 = 3.5 M_2$;
$x_1 = y_2 = 0$, $y_1 = y_3 = x_3 = 180^\circ$, $\cos x_2 = 0$
(R–matrix parameters: $\omega_j = x_j + i y_j$, $\omega_1 = \omega_{23}$, $\omega_2 = \omega_{13}$, $\omega_3 = \omega_{12}$**).**

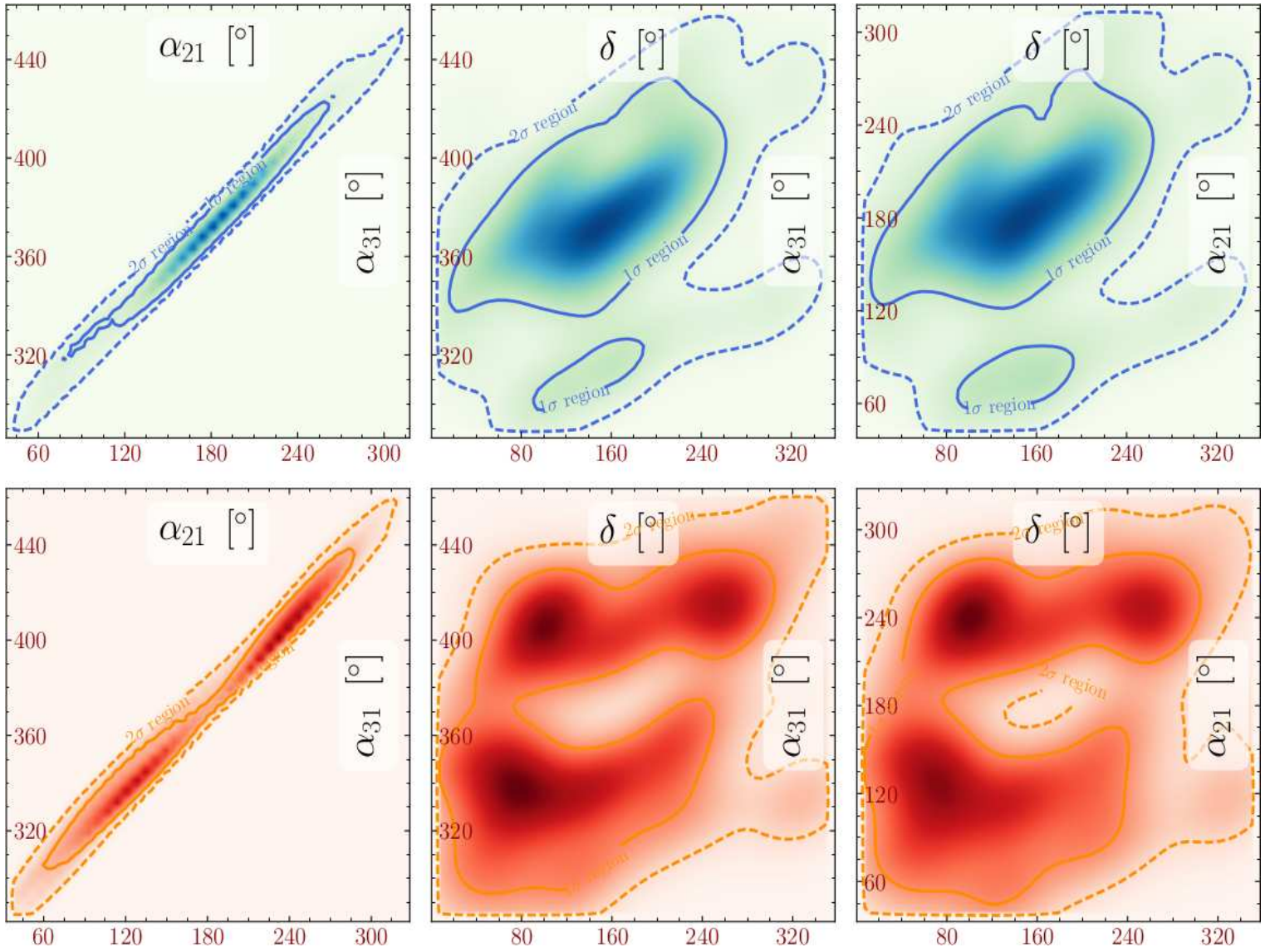

$M_1 = 1.29 \times 10^8$ **GeV.**

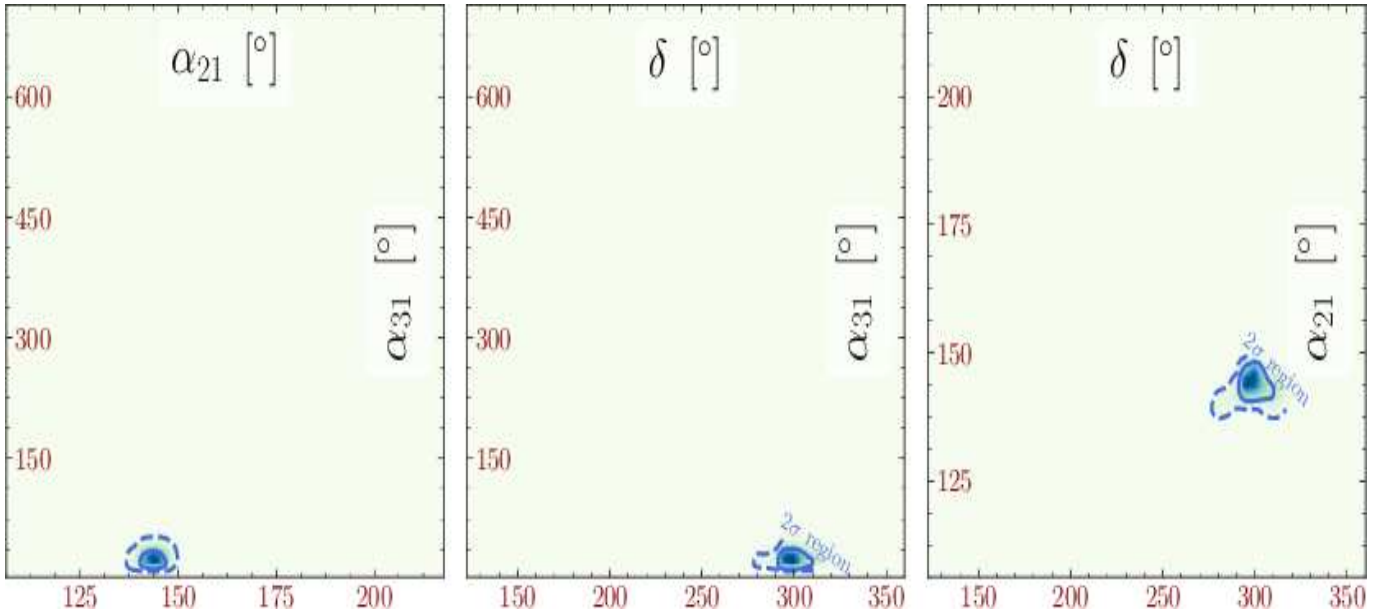

$M_1 = 3.16 \times 10^6$ **GeV,** $m_1 = 0.05$ **eV.**

Results presented also for $10^9 < M_1 < 10^{12}$ **GeV,** $9M_1 < 3M_2 < M_3$ **(**$M_1 << M_2$**).**

$m_1 = 0.0215$ **eV;** $x_1 = 90^\circ$, $x_3 = 180^\circ$, $y_2 = 0$, **chosen so that CP symmetry holds for** $\delta = 0$, $\alpha_{21} = 180^\circ$ **and** $\alpha_{21} = 0$ **(**$y_1 = y_3 = -33^\circ$, $x_2 = 18^\circ$**).**

i) Dirac CPV due to δ**;** $\alpha_{21} = 180^\circ$, $\alpha_{21} = 0^\circ$**.**

$\min(M_1) = 5.13 \times 10^{10}$ **GeV,** $M_2 = 2.19 \times 10^{12}$ **Gev,** $M_3 = 1.01 \times 10^{13}$ **GeV.**

ii) Majorana CPV due to α_{21}**:** $\delta = \alpha_{21} = 0^\circ$**.**

$\min(M_1) = 3.05 \times 10^{10}$ **GeV,** $M_2 = 10^{13}$ **Gev,** $M_3 = 3 \times 10^{13}$ **GeV.**

iii) Majorana CPV due to α_{31}**:** $\delta = 0$, $\alpha_{21} = 180^\circ$**.**

$\min(M_1) = 5.13 \times 10^{10}$ **GeV,** $M_2 = 10^{13}$ **Gev,** $M_3 = 3 \times 10^{13}$ **GeV.**

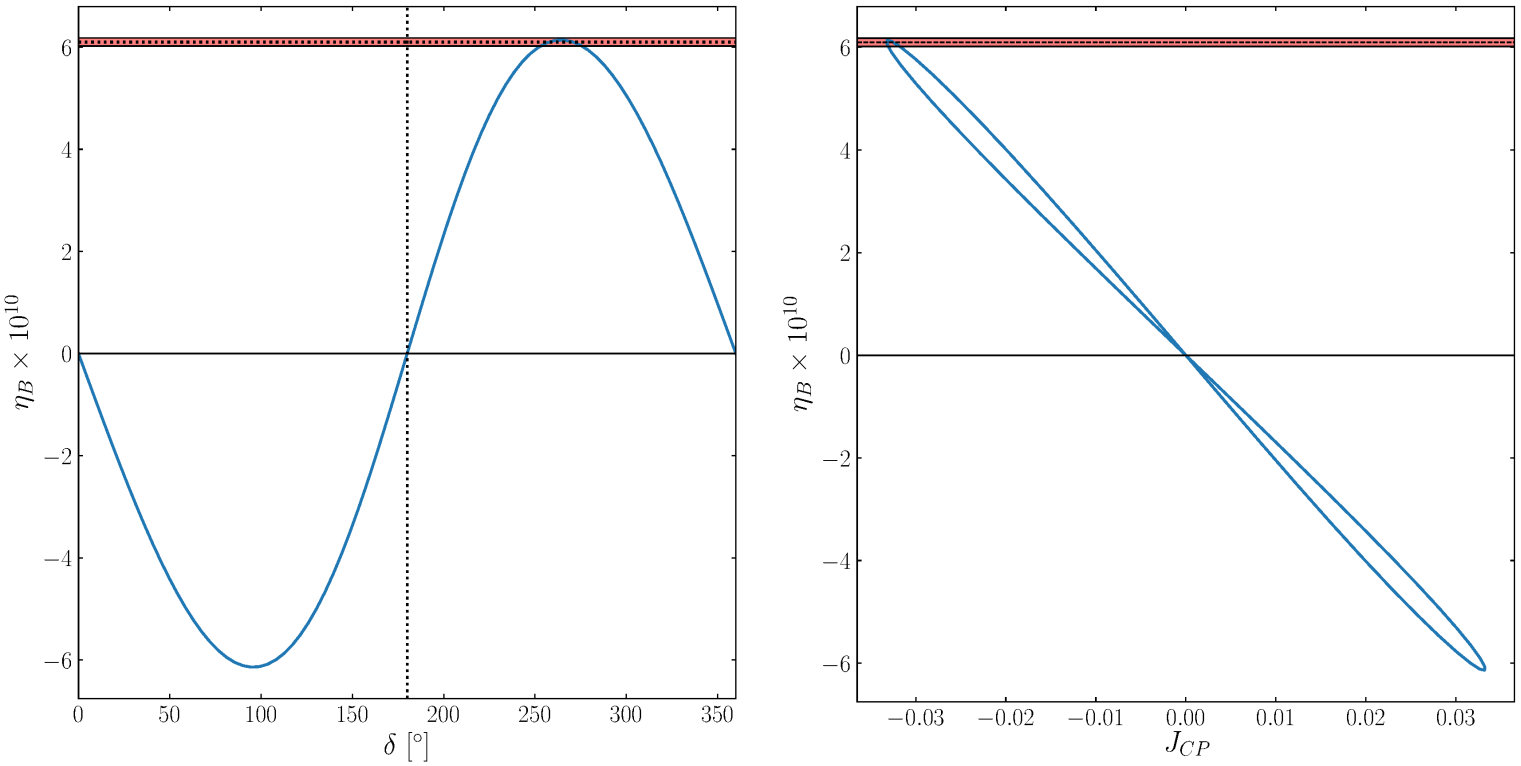

CP violation due to Dirac CPV δ:
$\min(M_1) = 5.13 \times 10^{10}$ GeV, $M_2 = 2.19 \times 10^{12}$ Gev,
$M_3 = 1.01 \times 10^{13}$ GeV;
$J_{CP} \cong -0.03$.

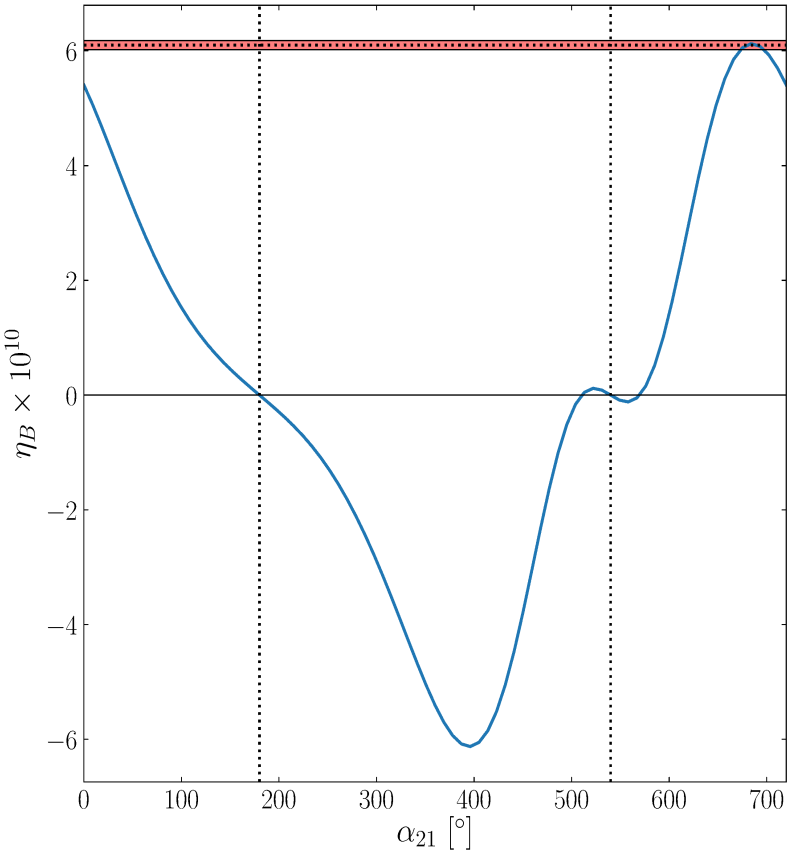

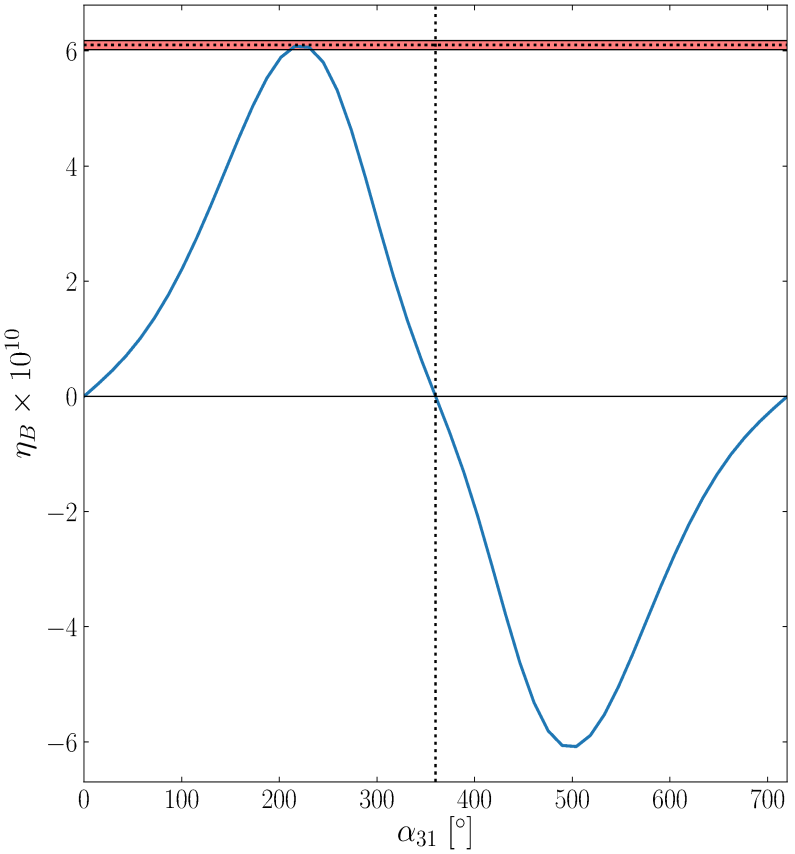

α_{21}: $\min(M_1) = 3.05 \times 10^{10}$ **GeV**, $M_2 = 10^{13}$ **Gev**, $M_3 = 3 \times 10^{13}$ **GeV**.

α_{31}: $\min(M_1) = 5.13 \times 10^{10}$ **GeV**, $M_2 = 10^{13}$ **Gev**, $M_3 = 3 \times 10^{13}$ **GeV**.

High Scale Transition

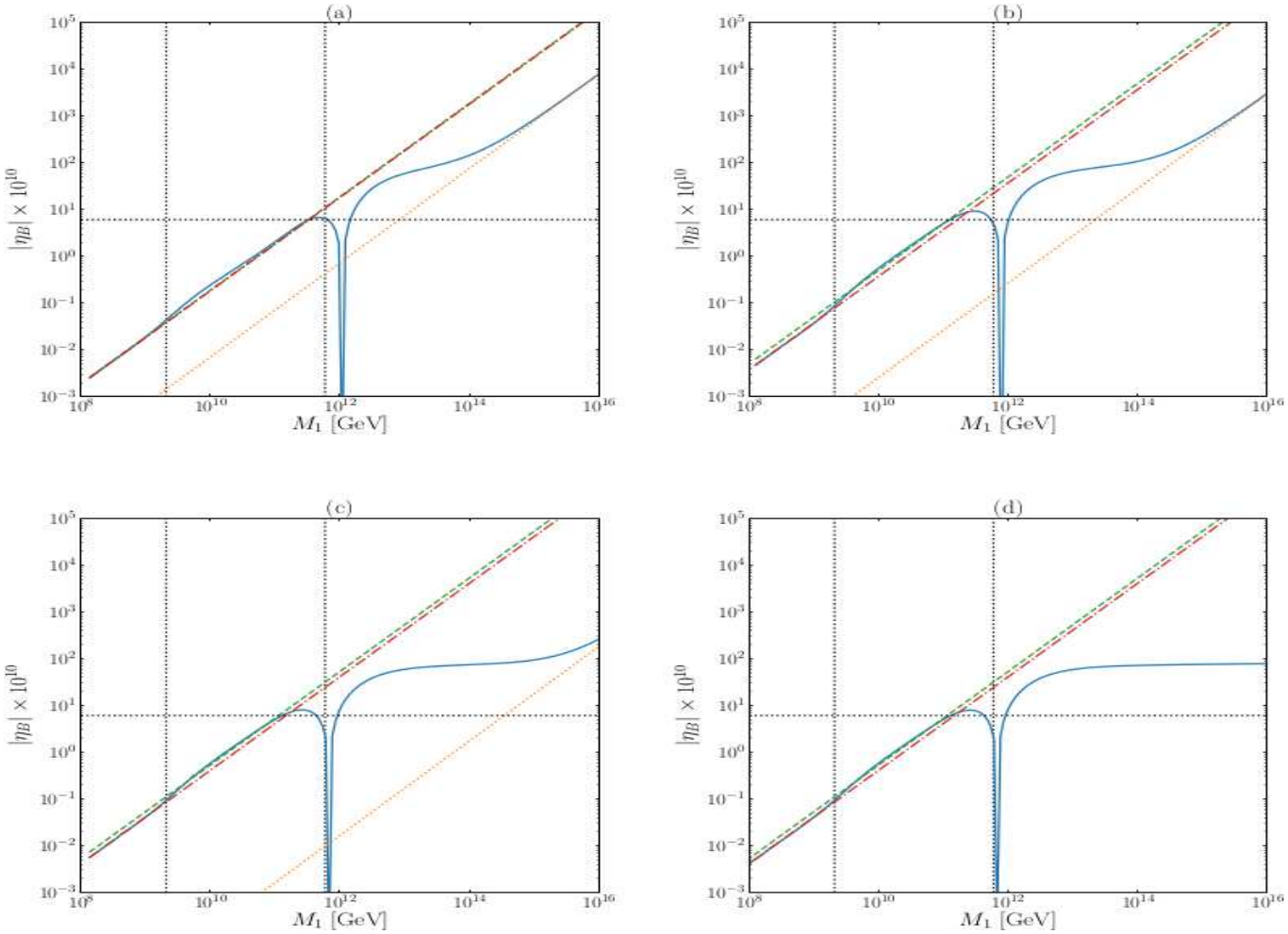

LG from M_1 ($M_1 << M_2 << M_3$): dashed green - 2-flavour BE; red dot-dashed - 3-flavour BE; dotted orange - single flavour BE; solid blue - solution of DME. y_3 - the only CPV $R-$ matrix parameter: $y_3 = 30^\circ$ (a), 5° (b), 0.3° (c), 0° (d). The vertical dotted lines: $M_1 = 10^9$ and 10^{12} GeV. Case d: CPV only from δ, α_{21}, α_{31}.

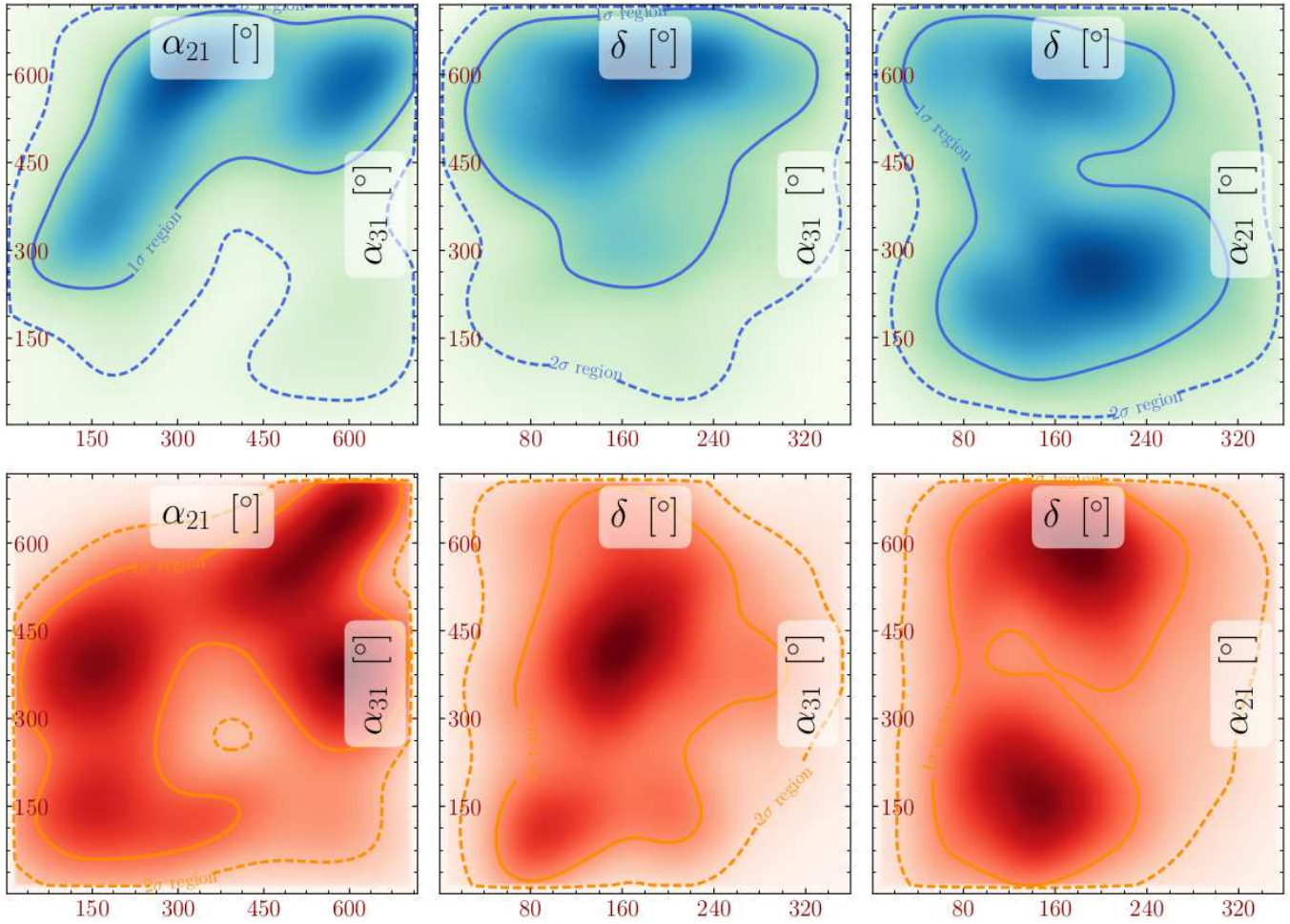

CP conserving $R-$ matrix ($y_j = 0$), CPV due to δ, α_{21} and α_{31}: $M_1 = 10^{13}$ GeV, $M_1 \ll M_2 \ll M_3$; $m_1 = 0.0159$ eV, NO; $x_1 = -96.55°$, $x_2 = -105.2°$ $x_3 = 141.4°$.

1BE1F: $\eta_B = 0$!.

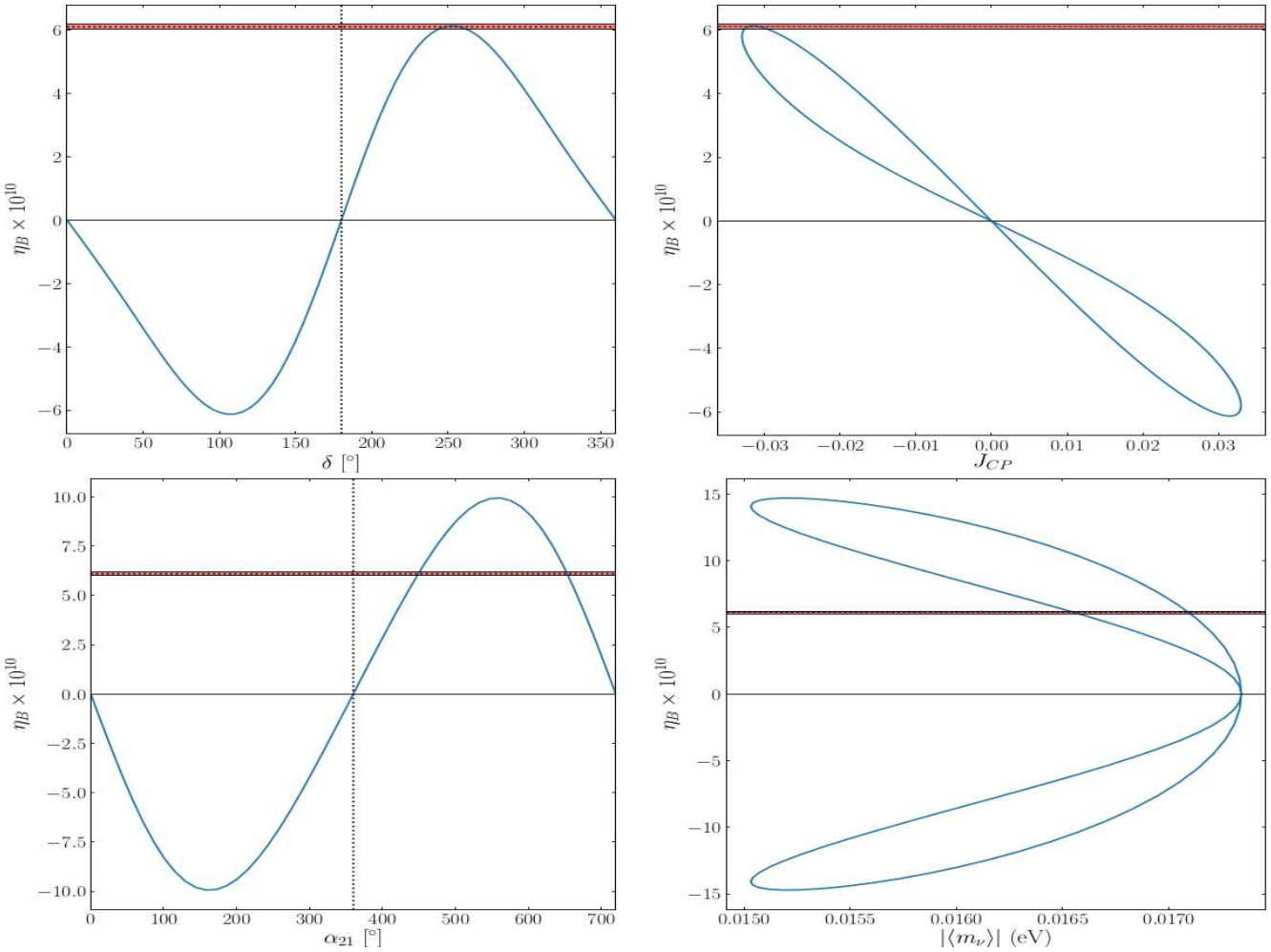

$M_1 = 3.16 \times 10^{13}$ **GeV, CP conserving** $R-$**matrix.**
δ**:** $\alpha_{21} = \alpha_{31} = 0$**, successful LG for** $\delta \cong 250°$**, for which** $J_{CP} \cong -0.03$**.**
α_{21}**:** δ**=**α_{31}**=0, successful LG for** α_{21}**=449°, 653°, for which** $|<m>|$ **=0.0171, 0.0166 eV.**

A. Granelli et al., arXiv:2107.02079: summary of the results.

Studied the transitions between different flavour regimes: $M_1 << M_2 << M_3$, CPV due to Dirac or Majorana CPV phases of the PMNS matrix. Used DME; the 1, 2 and 3 flavour regimes described by BE.

The 2 to 1 flavour LG transition taking place at $M_1 \sim 10^{12}$ GeV:
η_B goes through zero and changes sign in the transition
only in the strong wash-out regime and zero N_1 initial abundance..

Results on the 1 to 2 and 2 to 3 flavour regimes transitions in the case of $N_{1,2}$ with $M_1 << M_2$ (CP violation due to Dirac or Majorana CPV phases).
i) the BEs can fail to describe correctly the generation of η_B in the 1, 2 and 3 flavour regimes, e.g., underestimating η_B by a factor ~ 10;
ii) the 1-to-2 and the 2-to-3 flavour transitions can take place at the same M_1, with η_B going through a relatively shallow minimum at the transition value of M_1;
iii) the 2-flavour regime can persist above $5 \times 10^{11} - 10^{12}$ GeV (below $\sim 10^9$ GeV);
iv) the flavour effects in LG persist beyond $\sim 10^{12}$ GeV, with the requisite CPV provided by the Dirac or/and Majorana CPV phases;
v) at $M_1 \sim 10^{12}$ GeV, $|\eta_B|$ reaches a "plateau" where it remains practically constant as M_1 increases, and flavour effects are fully operative;
vi) determined $\min(M_1)$ and the ranges of δ and of $(\alpha_{21} - \alpha_{31})$ for which one can have successful LG;
vii) for NO spectrum, $\mathrm{sgn}(\sin\delta)$ is correlated with $\mathrm{sgn}(\eta_B)$ in the region of viable LG, with $\pi < \delta < 2\pi$ ($0 < \delta < \pi$) for real (purely imaginary) CP conserving Casas-Ibarra parameter $\sin 2\theta_{\mathrm{CI}}$;
for IO spectrum (viable LG possible only for purely imaginary $\sin 2\theta_{\mathrm{CI}}$) the same correlations holds for $4.6 \times 10^{10} \lesssim M_1 \lesssim 10^{13}$ GeV with $\pi < \delta < 2\pi$;
these results are testable in low-energy experiments.

Consider two-flavoured LG with $N_{1,2,3}$, $M_1 \ll M_2 \ll M_3$, $M_1 10^9$ GeV. Only the CPV decays of N_1 contribute to the generation of CPV lepton asymmetry which is converted into a baryon asymmetry by the sphaleron effects. The DMEs describe the evolution of the number of N_1 in a comoving volume, N_{N_1}, and of the CPV asymmetries in the lepton charges L_τ and $L_{\tau^\perp} = L_{e+\mu} = L_e + L_\mu$.
The $B-L$ asymmetry $N_{B-L} = N_{\tau\tau} + N_{\tau^\perp\tau^\perp}$ is given by:

$$N_{B-L}(z_f) = N^{\rm 1BE1F}_{B-L}(z_f) + N^{\rm decoh}_{B-L}(z_f)\,,$$

$$N^{\rm 1BE1F}_{B-L}(z) \equiv \int_{z_0}^{z} e^{-\int_{z'}^{z_f} W_1(z'')dz''} \epsilon^{(1)} D_1(z')(N_{N_1}(z') - N^{eq}_{N_1}(z'))\,dz'\,, \quad z_0 = 10^{-3}\,,$$

is the solution to the 1BE1F. It vanishes if CPV in LG is due to δ and/or $\alpha_{21,31}$ since in this case $\epsilon^{(1)} = \epsilon^{(1)}_{\tau\tau} + \epsilon^{(1)}_{\tau^\perp\tau^\perp} = \epsilon^{(1)}_{\tau\tau} + \epsilon^{(1)}_{ee} + \epsilon^{(1)}_{\mu\mu} = 0$.
$N^{\rm decoh}_{B-L}$ incorporates the decoherence effects due to Γ_τ. At $M_1 > 10^{12}$ GeV, to leading order in $\Lambda_\tau \equiv \Gamma_\tau/Hz = $ const.$/M_1$,

$$N_{B-L}(z_f) = \Lambda_\tau \mathcal{I}_2(\kappa_1; z_f)(1 - 2p_{1\tau})\epsilon^{(1)}_{\tau\tau} + \mathcal{O}(\Lambda^2_\tau)\,, \quad p_{1\tau} = |C_{1\tau}|^2 = |Y_{\tau 1}|^2/(Y^\dagger Y)_{11}\,,$$

$\mathcal{I}_2(\kappa_1; z_f)$ does not depend on M_1, $\epsilon^{(1)} \propto M_1$, $\Lambda_\tau \propto 1/M_1$, thus $N_{B-L}(z_f)$ is constant with M_1. At $M_1 > 10^{12}$ GeV there should exist an interval of values of M_1 in which η_B does not change with M_1.
The numerical solutions of the DMEs show the existence of a plateau at $M_1 > 10^{12}$ GeV.

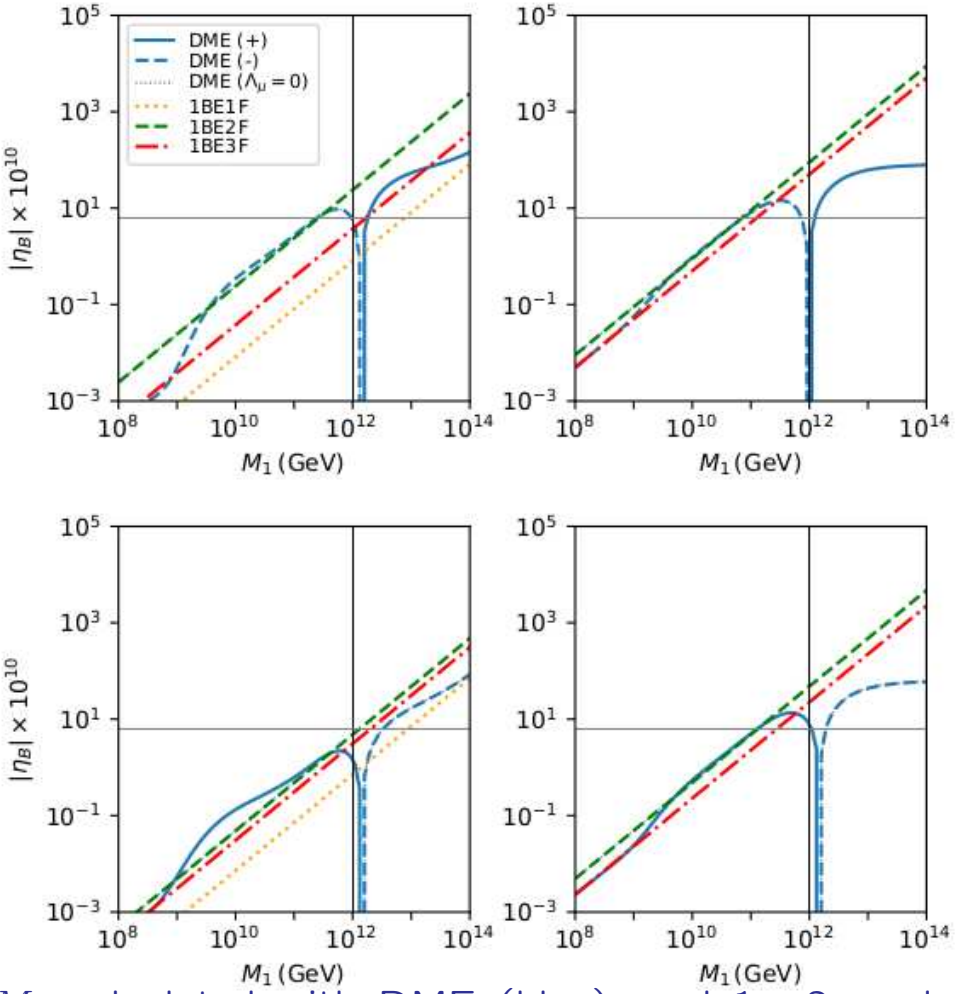

$|\eta_B|$ as a function of M_1 calculated with DME (blue), and 1-, 2- and 3-flavoured Boltzmann equations 1BE1F (orange dotted), 1BE2F (green dashed) and 1BE3F (red dash-dotted). The solid (dashed) blue curve corresponds to $\eta_B > 0$ ($\eta_B < 0$), while the dotted blue curve is obtained for $\Lambda_\mu = 0$. The relevant parameters are set to: $M_3 = 5M_2 = 50M_1$, $\delta = 228^\circ$, $\alpha_{21} = 200^\circ$, $\alpha_{31} = 175^\circ$, $x_1 = -/+10^\circ$, $x_2 = -/+20^\circ$, $x_3 = -/+10^\circ$ in the top/bottom panels and $y_1 = y_2 = 0$ and $y_3 = 30^\circ/0$ in the left/right panels. In the top-right and bottom-right panels the CPV is due only to the CPV phases in the PMNS matrix ($y_{1,2,3} = 0$), so the 1BE1F solution $\eta_B^{1BE1F} = 0$. The horizontal (vertical) grey (black) line corresponds to the observed η_B (to $M_1 = 10^{12}$ GeV).

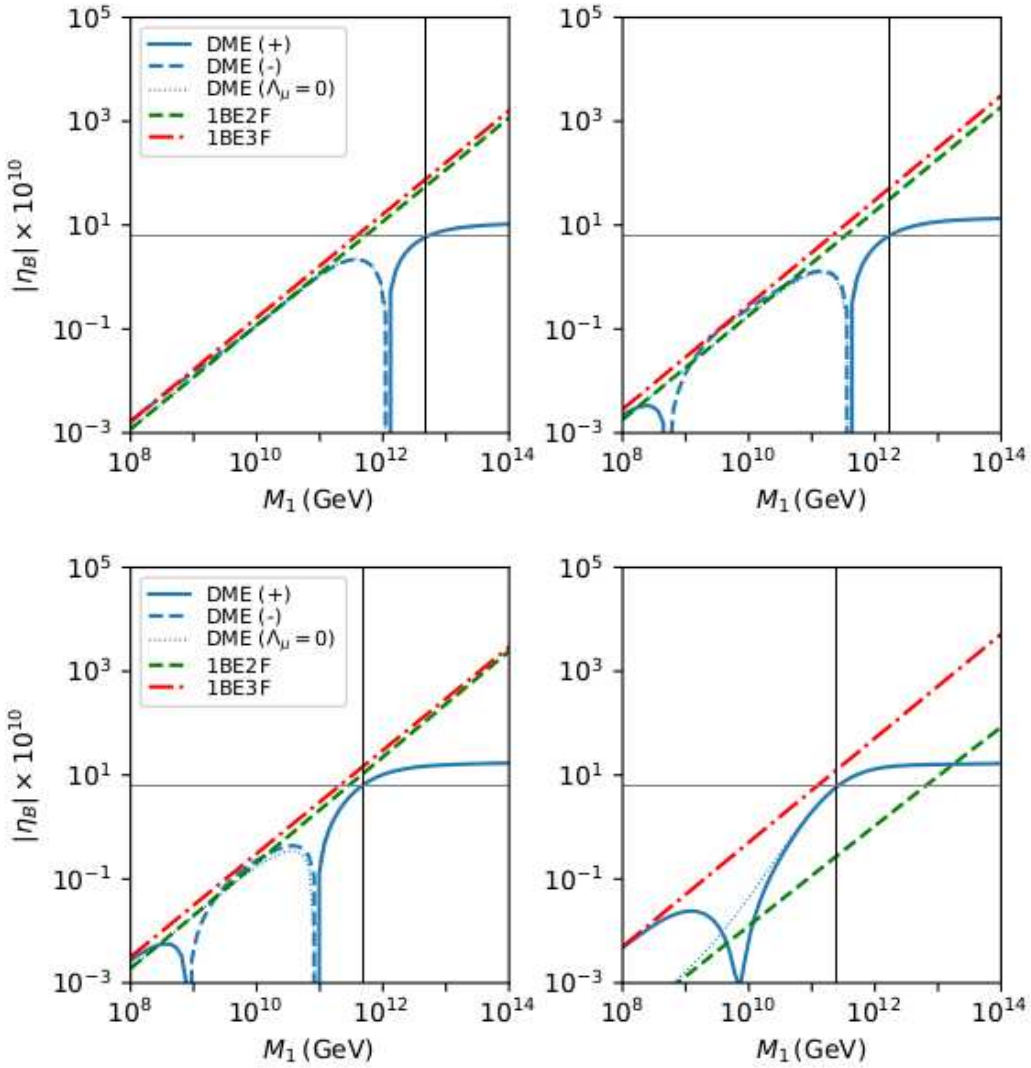

$|\eta_B|$ versus M_1 for NH spectrum, obtained with DME (blue), 1BE2F (green), 1BE3F (red), for $\delta = 3\pi/2$, $\alpha_{23} = 0$, $x = 150°/40°$ (top left/right panels) and $30°/22.2°$ (bottom left/right panels). The solid (dashed) blue line corresponds to $\eta_B > 0$ ($\eta_B < 0$); the dotted blue line is obtained for $\Lambda_\mu = 0$. The horizontal grey line marks the present BAU at 6.1×10^{-10} and is reproduced with the solution of DMEs at the minimal mass scales marked by the vertical black line, i.e., at $M_1 \simeq 4.7/1.7 \times 10^{12}$ GeV top-left/right panels and $4.8/2.5 \times 10^{11}$ GeV bottom-left/right panels.

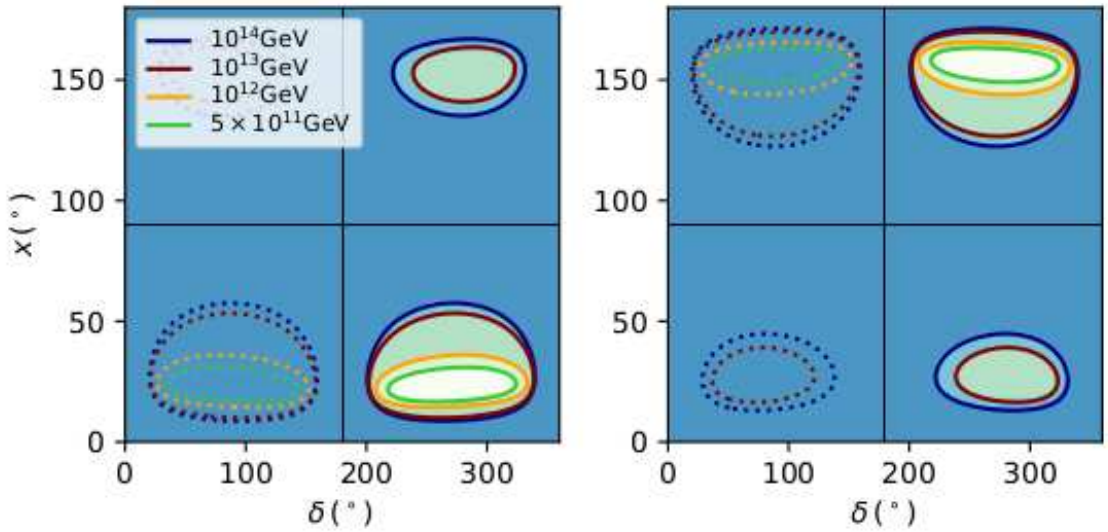

Regions of viable leptogenesis in the $\delta - x$ half plane, $0 \leq x \leq \pi$ ($\theta_{\rm CI} = x + iy$), for NH spectrum, real R-matrix ($y = 0$), CP violation due to the Dirac phase δ, $\alpha_{23} = 0$ (left panel) and 2π (right panel) and different values of M_1. The solid contours corresponding to fixed values of M_1 surround the regions in which there is a combination of values of δ and x for which $\eta_B = 6.1 \times 10^{-10}$. The dotted contours surround regions where one can have $|\eta_B| = 6.1 \times 10^{-10}$ but $\eta_B < 0$. The predicted η_B outside the contours is always smaller in magnitude than the observed BAU. The regions of viable leptogenesis in the half-plane $-\pi \leq x \leq 0$ (or $\pi \leq x \leq 2\pi$), which are not shown, can be obtained from those in the figure by substituting x with $x - \pi$.

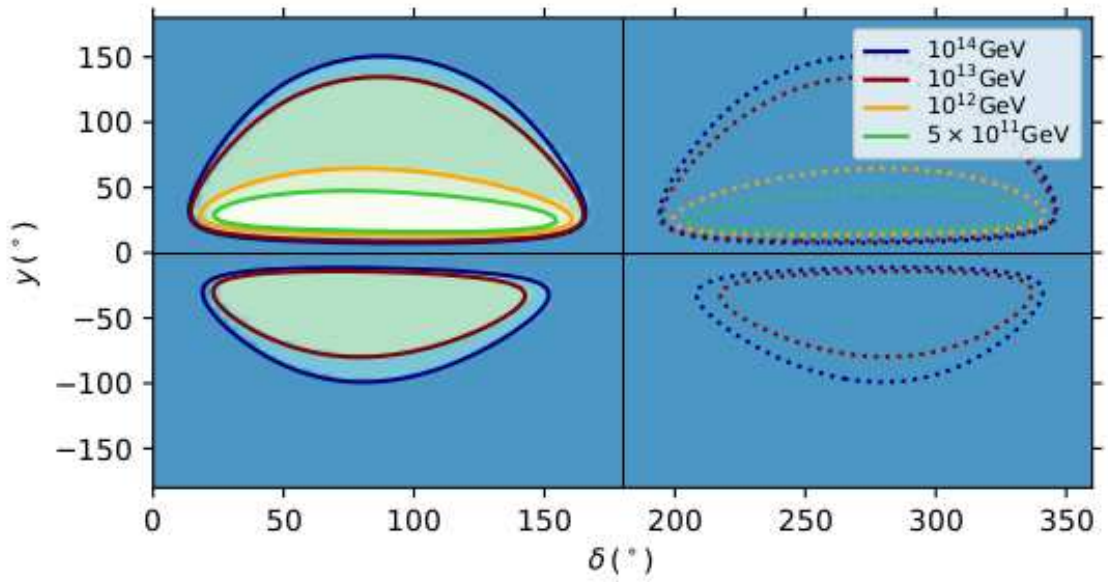

Regions of viable leptogenesis in the $\delta - y$ plane for NH spectrum, $x = k\pi$, $k = 0, 1, 2$ ($\theta_{\rm CI} = x + iy$), $\alpha_{23} = \pi$, i.e., CP violation due to δ ($y \neq 0$, CP-conserving R-matrix) and different M_1. The solid contours corresponding to fixed values of M_1 surround the regions in which there is a combination of values of δ and y for which $\eta_B = 6.1 \times 10^{-10}$. The dotted contours surround regions where one can have $|\eta_B| = 6.1 \times 10^{-10}$ but $\eta_B < 0$. The predicted η_B outside the contours is smaller in magnitude than the present BAU. Setting $\alpha_{23} = 3\pi$ leads to a figure which can be obtained from the present by changing y to $-y$.

I. Brivio et al, arXiv:1905.12642

C. Is leptogenesis compatible with the Neutrino Option?

The Neutrino Option

$$V_0(\Phi) = -\frac{M_{H0}^2}{2}\Phi^\dagger\Phi + \lambda_0(\Phi^\dagger\Phi)^2,$$

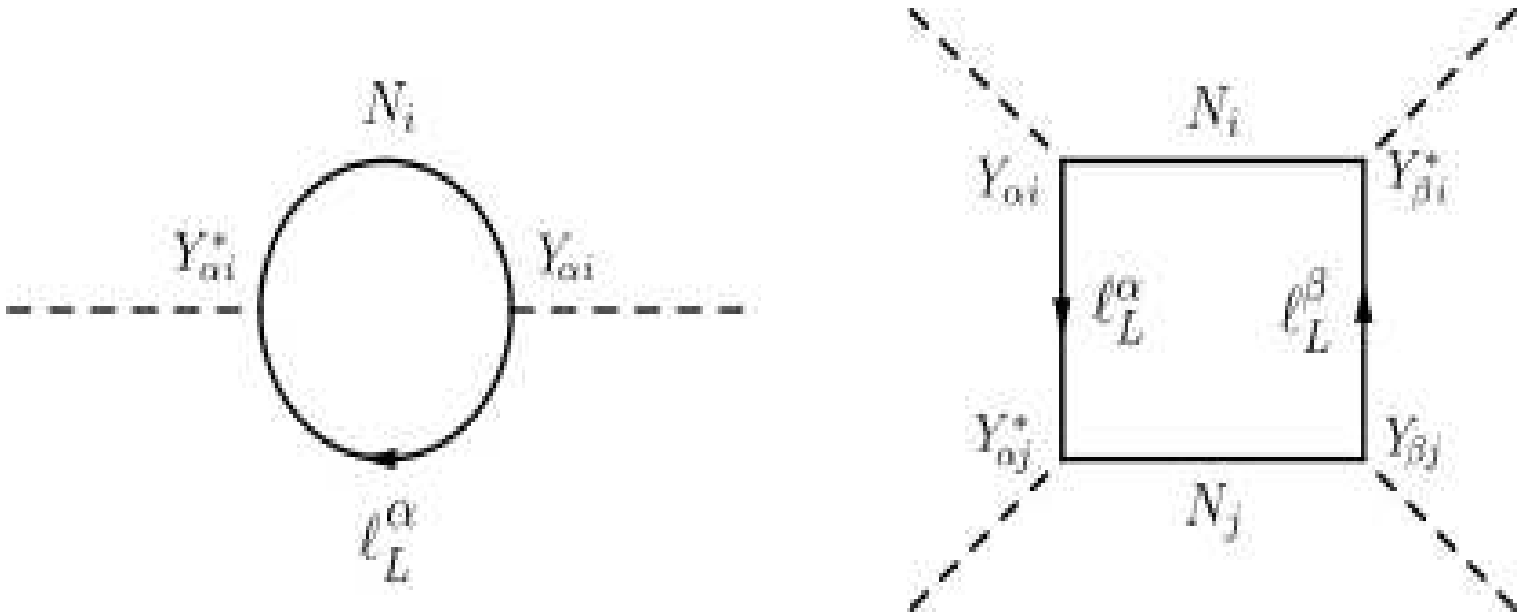

I. Brivio and M. Trott, 2017 (arXiv:1703.10924

$$\Delta M_H^2 = \frac{1}{8\pi^2}\textbf{Tr}\left[Y M^2 Y^\dagger\right].$$

Our analysis:

M_{H0}^2 **generated at one loop,** λ_0**-present in** $V_0(\Phi)$**.**

Successful LG possible in the resonant regime.

The case of 2 heavy Majorana N_j **considered:** $N_{1,2}$**,** $N_{1,2}$ **form a pseudo-Dirac pair,** $M_2 - M_1 \ll M_{1,2}$**.**

$$M_{H0}^2 = \Delta M_H^2 = \frac{1}{8\pi^2 v^2}\cosh(2y) M^3 (m_1 + m_2 + m_3),$$

R**:** $R_{12} = \cos\theta$**,** $R_{13} = \sin\theta$**,** $R_{22} = -\sin\theta$**,** $R_{23} = \cos\theta$**,**
NO spectrum, $\theta = x + iy$**.**

The Neutrino Option and successful LG are compatible in the case of a NO (IO) neutrino mass spectrum for

$1.2 \times 10^6 < M$ **(GeV)** $< 8.8 \times 10^6$
($2.4 \times 10^6 < M$ **(GeV)** $< 7.4 \times 10^6$**),** $M = (M_1 + M_2)/2$**.**

Successful leptogenesis requires that $\Delta M/M \equiv (M_2 - M_1)/M \sim 10^{-8}$**.**

LG can produce the BAU within the Neutrino Option scenario when the requisite CP violation in LG is provided exclusively by the Dirac or Majorana low energy CPV phases of the PMNS matrix.

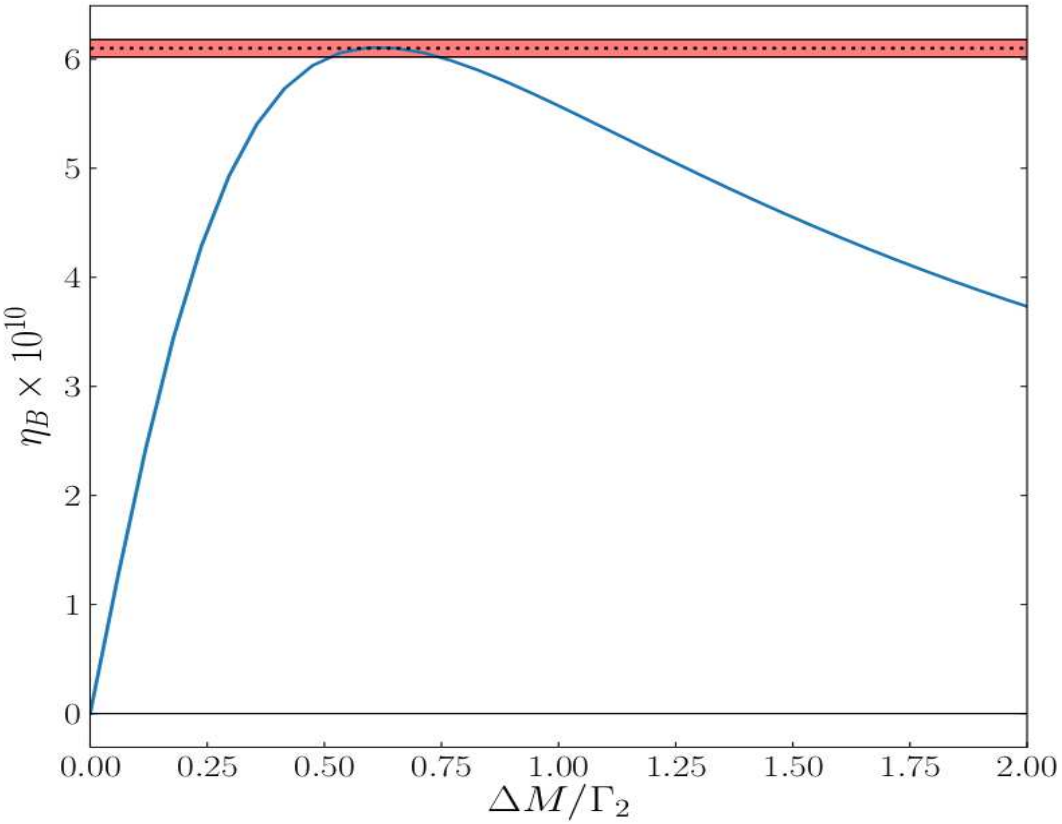

$\Gamma_2 = 1.62 \times 10^{-2}$ (8.63×10^{-3}) **GeV for NO (IO) spectrum.**

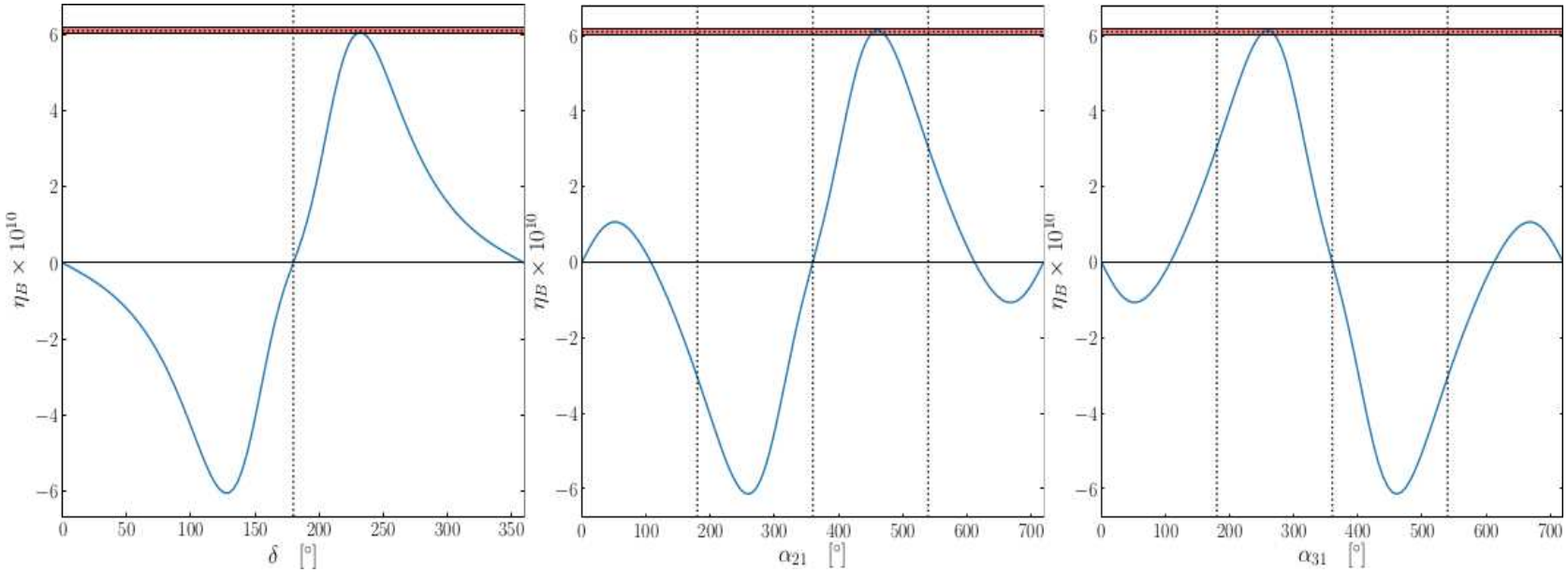

$M = 8 \times 10^6$ **GeV**

Conclusions.

The see-saw mechanism provides a link between the ν-mass generation and the baryon asymmetry of the Universe (BAU).

Any of the CPV phases in $U_{\rm PMNS}$ can be the leptogenesis CPV parameters.

Low energy leptonic CPV can be directly related to the existence of BAU.

Understanding the status of the CP-symmetry in the lepton sector is of fundamental importance.

These results underline further the importance of the experimental studies on Dirac and/or Majorana leptonic CP-violation at low energies.